

SHAPR Predicts 3D Cell Shapes from 2D Microscopic Images

Dominik J. E. Waibel^{1,2}

Niklas Kiermeyer¹

Scott Atwell⁴

Ario Sadafi¹

Matthias Meier⁴

Carsten Marr¹

DOMINIK.WAIBEL@HELMHOLTZ-MUENCHEN.DE

NIKLAS.KIERMEYER@HELMHOLTZ-MUENCHEN.DE

SCOTT.ATWELL@HELMHOLTZ-MUENCHEN.DE

ARIO.SADAFI@HELMHOLTZ-MUENCHEN.DE

MATTHIAS.MEIER@HELMHOLTZ-MUENCHEN.DE

CARSTEN.MARR@HELMHOLTZ-MUENCHEN.DE

¹ Institute of AI for Health, Helmholtz Munich, Neuherberg, Germany ² Technical University of Munich, School of Life Sciences, Weihenstephan, Germany ³ Computer Aided Medical Procedures, Technical University of Munich, Munich, Germany ⁴ Helmholtz Pioneer Campus, Helmholtz Munich, Neuherberg, Germany

Abstract

Reconstructing shapes of three-dimensional (3D) objects from two-dimensional (2D) images is a challenging spatial reasoning task for both our brain and computer vision algorithms. We focus on solving this inverse problem with a novel deep learning SHApe PRediction autoencoder (SHAPR), and showcase its potential on 2D confocal microscopy images of single cells and nuclei. Our findings indicate that SHAPR reconstructs 3D shapes of red blood cells from 2D images more accurately than naïve stereological models and significantly increases the feature-based classification of red blood cell types. Applying it to 2D images of spheroidal aggregates of densely grown human induced pluripotent stem cells, we observe that SHAPR learns fundamental shape properties of cell nuclei and allows for prediction-based 3D morphometry. SHAPR can help to optimize and up-scale image-based high-throughput applications by reducing imaging time and data storage.

Keywords: 3D shape prediction, stereology, single-cell morphometry, adversarial learning

1. Introduction

Recording single cells in three dimensions (3D) for high-throughput biomedical applications is prohibitively time-consuming as it requires imaging multiple slices, raising the question how to optimally trade-off between throughput and resolution in space and time. While deep learning-based solutions for predicting 3D object shapes from photographs exist (Wang et al., 2018; Kaiming et al., 2017; Choy et al., 2016) for airplanes, cars, and furniture, they cannot be directly translated to biomedical applications in particular. Fluorescence microscopy images differ substantially from real-world photographs in terms of color, contrast, and object orientation, thus requiring specialized approaches. Shapes of single cells are often similar but never the same and in the biomedical domain the number of training images is orders of magnitude smaller than for objects in photographs.

2. Results

We addressed these problems with SHAPR, a novel deep learning autoencoder architecture (Figure 1a), that is complemented with a discriminator model ¹. Five independent SHAPR

1. Open source code and documentation: <https://github.com/marrlab/SHAPR>

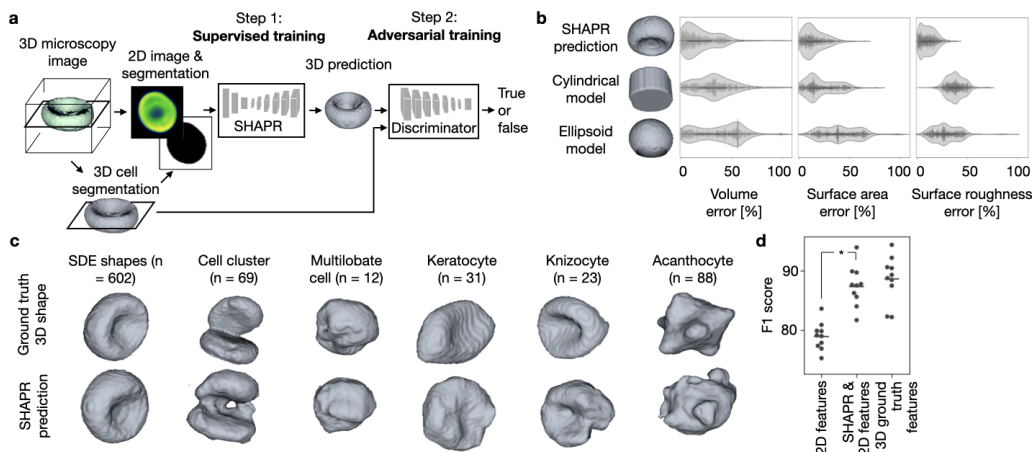


Figure 1: SHAPR predicts 3D red blood cell shapes from 2D microscopic images. **a**, SHAPR consists of an autoencoder and discriminator using a two-step training approach, **b**, and significantly outperforms naïve stereological models. **c**, Example predictions of red blood cells from six different classes. **d**, Random forest-based classification significantly improves when morphological features from SHAPR predictions are added to features from 2D images.

models were trained on each dataset with a combination of binary cross entropy and dice loss in a round-robin fashion, so each input image was contained in the test set exactly once, with a 20% test set, 20% validation set split, using the remaining data as a training set. For proof of concept, we predicted 825 3D red blood cell shapes (Simionato et al., 2021) from 2D images that intersect the red blood cell at the center slice, adding the corresponding 2D segmentation. SHAPR predictions significantly outperformed two naïve stereological models, i.e. a cylindrical and an ellipsoid fit (Figure 1b), serving as a baseline, in terms of relative volume error ($V_{SHAPR}=20\pm 18\%$, $V_{cylindrical}=33\pm 22\%$, $p_{cylindrical}=2.6\times 10^{-46}$; and $V_{ellipsoid}=37\pm 23\%$; $p_{ellipsoid}=7.8\times 10^{-73}$, $n=825$, paired Wilcoxon signed-rank test).

Strikingly, enriching 2D features with SHAPR derived morphological features a random-forest classification task, assigning each blood cell to one of six classes, led to a significantly better performance ($F1=87.4\pm 3.1\%$, mean \pm std.dev., $n=10$ cross-validation runs) than using 2D features only ($F1=79.0\pm 2.2\%$), $p=0.005$, paired Wilcoxon signed-rank test). Because predicting shapes from 2D planes close to the cell’s center of mass does not accurately reflect the complexity of real world applications, we challenged SHAPR to predict 3D cell nuclei from confocal z-stacks containing 887 fluorescence stained nuclei from six manually segmented human-induced pluripotent stem cells cultured in a spheroidal aggregate. SHAPR was provided with nuclei from one 2D slice through the aggregate, thus nuclei were cut at random heights, complicating the prediction task (Figure 2). Again, the relative volume error was significantly lower for SHAPR ($V_{SHAPR}=33\pm 41\%$ vs. $V_{cylindrical}=44\pm 25\%$, $p_{cylindrical}=9.2\times 10^{-36}$, and $V_{ellipsoid}=62\pm 29\%$, $p_{ellipsoid}=8.7\times 10^{-86}$, $n=887$, paired Wilcoxon signed-rank test) compared to the naïve models. While the naïve models simply extrapolated the area to volume monotonically, the ground truth suggests a more complex relationship, which SHAPR captured.

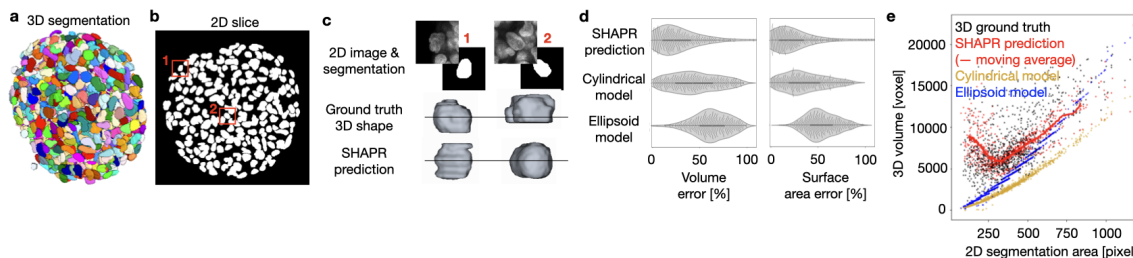


Figure 2: SHAPR learns fundamental 3D shape properties of human-induced pluripotent stem cell nuclei from a single 2D slice. **a**, Representative image of one manually segmented aggregate. **b**, **c**, 2D nuclei examples from a single slice and fluorescent images of the intersecting slice. **d**, SHAPR predictions outperform naïve models, which only extrapolate volumes, (**e**) whereas SHAPR has learned complex, non-linear relations between the 2D segmentation area and the 3D volume of a nucleus.

3. Discussion

SHAPR is able to solve the ambiguous inverse problem of predicting 3D shapes of single cells and nuclei from 2D images, as we have shown on two different datasets. Unlike Wu et. al.’s (Wu et al., 2019) approach SHAPR does not refocuss fluorescent signal onto a user defined surface but performs an inverse spatial reasoning task, considering contextual information. As a general open-source deep learning architecture SHAPR is not limited to confocal fluorescence images, therefore we believe that this opens the door towards other applications. Predicting 3D shapes from 2D images thus offers a simple way to reduce imaging time and data storage while retaining morphological details. Beyond single-cell shape prediction, SHAPR may be extended to other biological structures, including organelles and proteins, and may increase the efficiency of biomedical imaging in multiple domains.

References

- Christopher B Choy, Danfei Xu, Junyoung Gwak, Kevin Chen, and Silvio Savarese. 3D-R2N2: A unified approach for single and multi-view 3D object reconstruction. In *Computer Vision – ECCV 2016*, pages 628–644. Springer International Publishing, 2016.
- He Kaiming, Gkioxari Georgia, Dollar Piotr, and Girshick Ross. Mask r-cnn. In *International conference on computer vision*, volume 1, 2017.
- Greta Simionato, Konrad Hinkelmann, Revaz Chachanidze, Paola Bianchi, Elisa Fermo, Richard van Wijk, Marc Leonetti, Christian Wagner, Lars Kaestner, and Stephan Quint. Red blood cell phenotyping from 3D confocal images using artificial neural networks. *PLoS Comput. Biol.*, 17(5):e1008934, May 2021.
- Nanyang Wang, Yinda Zhang, Zhuwen Li, Yanwei Fu, Wei Liu, and Yu-Gang Jiang. Pixel2mesh: Generating 3d mesh models from single rgb images. In *Proceedings of the European Conference on Computer Vision (ECCV)*, pages 52–67, 2018.
- Yichen Wu, Yair Rivenson, Hongda Wang, Yilin Luo, Eyal Ben-David, Laurent A Bentolila, Christian Pritz, and Aydogan Ozcan. Three-dimensional virtual refocusing of fluorescence microscopy images using deep learning, 2019.